The Effect of Timing Jitter on the Performance of a Discrete Multitone System

T. Nicholas Zogakis, *Member, IEEE*, and John M. Cioffi, *Fellow, IEEE*

***Abstract*— The transmission of high-speed data over severely band-limited channels may be accomplished through the use of discrete multitone (DMT) modulation, a modulation technique that has been proposed for a number of new applications. While the performance of a DMT system has been analyzed by a number of authors, these analyses ignore the effect of timing jitter on system performance. Timing jitter becomes an increasingly important concern as higher data rates are supported and larger constellations are allowed on the DMT subchannels. Hence, in this paper, we assume that synchronization is maintained by using a digital phase-locked loop to track a pilot carrier. Given this model, we derive error rate expressions for an uncoded DMT system operating in the presence of timing jitter, and we derive an expression for the interchannel distortion that results from a varying timing offset across the DMT symbol. In addition, we investigate the performance of trellis-coded DMT modulation in the presence of timing jitter. Practical examples from the asymmetric digital subscriber line (ADSL) service are used to illustrate various results.**

I. Introduction

DISCRETE multitone (DMT) modulation is a technique in which a transmission channel is partitioned into a number of independent, parallel subchannels, each of which may be considered as supporting a lower-speed quadrature amplitude modulated (QAM) signal [1]. Performance is maximized by allocating more bits to subchannels with high signal-to-noise ratios (SNR's) and fewer or no bits to subchannels with low SNR's. An example of an application for which DMT modulation is well suited is the asymmetric digital subscriber line (ADSL), a service proposed for providing a high-speed downstream channel, ranging from 1.544 Mb/s to 6.4+ Mb/s, from the central office to the customer, along with a lower-speed upstream channel over existing copper twisted pair [2].

Several authors have evaluated the performance of a DMT system for a variety of applications, focusing on maximizing data rate or maximizing margin under a constraint on the available transmit power [1], [3]–[5]. However, in these analyses, perfect synchronization is assumed, whereas in an actual system, the practical timing recovery mechanism will result in some degree of timing jitter. The importance of this form of impairment in the determination of error rate performance increases as the available bandwidth, which is determined by the channel SNR function, decreases and as the data rate increases, since both trends result in larger constellations being used on some of the subchannels. When large spectral efficiency is required and constellations supporting on the order of 10 b or more are allowed, then careful attention must be given to the synchronization scheme.

Similar to more traditional single-carrier modulation techniques, the performance of a DMT system may be enhanced by the application of coding. For instance, [6] and [7] present methods for applying trellis coding to DMT modulation, while [8] investigates the performance of a concatenated coding scheme consisting of an inner trellis code and outer Reed–Solomon code when applied to a DMT system. Each of these coding schemes requires constellation expansion over a subset of the carriers and, thus, potentially increases the susceptibility of the system to timing jitter. Furthermore, trellis decoders are based on the assumption of uncorrelated Gaussian noise, whereas, timing jitter introduces correlated noise into the system. For a DMT system employing trellis coding across the tones as described in [7], the correlation between the phase errors caused by timing jitter on consecutive complex symbols at the input to the trellis decoder is quite strong. Hence, it is not clear whether or not the timing jitter requirements are significantly tighter for a trellis-coded DMT system compared to an uncoded DMT system.

In this paper, we investigate the performance of both an uncoded and a trellis-coded DMT system in the presence of timing jitter. For simplicity, we assume that synchronization is maintained by designating one of the carriers as a pilot signal and using a digital phase-locked loop in the receiver to track the pilot carrier. This assumption leads to a tractable analysis and corresponds to the technique implemented in DMT modems for ADSL. Throughout the analysis, examples from the ADSL service are used to illustrate various points.

In Section II, we establish the DMT timing jitter model that serves as a starting point for the analysis. In Section III, we analyze the performance of an uncoded DMT system in the presence of timing jitter, and we compare the analytical results to simulation results for two ADSL scenarios. In Section IV, we first address the application of trellis coding to DMT modulation and then investigate the performance of a trellis-coded DMT system in the presence of timing jitter. Finally, in Section V, we discuss some of the implications of our results for the ADSL service.

Paper approved by P. H. Wittke, the Editor for Communication Theory of the IEEE Communications Society. Manuscript received August 15, 1994; revised July 15, 1995. This work was supported in part by a National Science Foundation (NSF) Fellowship and in part by Contracts CASIS 2DPD335 and NSF 2DPL133.

T. N. Zogakis was with the Information Systems Laboratory, Stanford University, Stanford, CA 94305 USA. He is now with Amati Communications Corporation, Mountain View, CA 94040 USA.

J. M. Cioffi is with the Information Systems Laboratory, Stanford University, Stanford, CA 94305 USA.

Publisher Item Identifier S 0090-6778(96)05506-7.

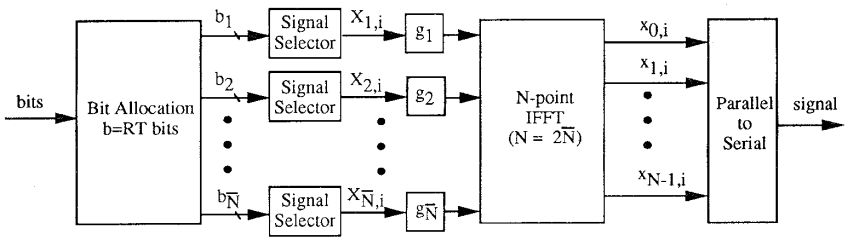

Fig. 1. Baseline DMT transmitter.

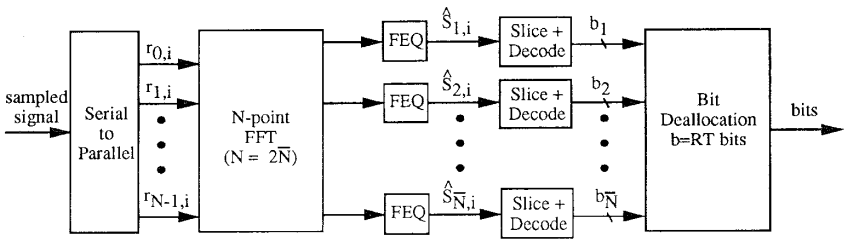

Fig. 2. Baseline DMT receiver.

II. DMT Timing Jitter Model

Figs. 1 and 2 present simplified block diagrams of the DMT system that we consider in this paper. At the input to the transmitter, the bit stream is partitioned into blocks of size $b = RT$ bits, where R is the uncoded bit rate, T is the DMT symbol period, and b is the number of bits contained in one DMT symbol. The bits collected during the ith symbol interval are allocated among $\overline{N}$ subchannels or tones in a manner determined during system initialization, with b_k bits assigned to tone k and $\Sigma\ b_k = b$. On subchannel k, the b_k bits are mapped to a constellation point $X_{k,i} = A_{k,i} + jB_{k,i}$ in a constellation of size 2^{b_k} with unity distance between constellation points. Next, the constellation point is scaled by a real multiplier, g_k, and the collection of constellation points $\{\overline{X}_{k,i} = g_k X_{k,i}, k = 1, \cdots, \overline{N}\}$ serves as the input to an inverse fast Fourier transform (IFFT) block. The constants $\{g_k\}$ are chosen so that $E\{|\overline{X}_{k,i}|^2\} = P_k$, the power allocated to the kth tone. The time-domain signal that is transmitted over the channel is obtained by performing a length $N = 2\overline{N}$ IFFT on the complex symbols $\{\overline{X}_{k,i}, k = 0, 1, \cdots, N-1\}$, where $\overline{X}_{0,i} = 0$ and $\{\overline{X}_{k,i} = \overline{X}^*_{N-k,i}, k = \overline{N}+1, \overline{N}+2, \cdots, N-1\}$.[1]

The kth subchannel is associated with the frequency $f_k = k\Delta f$, where $\Delta f = 1/T$. Hence, the DMT symbol transmitted during the ith symbol period is given by [9], [11]

$$y_i(t) = \frac{2}{\sqrt{N}} \sum_{k=1}^{N/2-1} [\overline{A}_{k,i} \cos(2\pi k \Delta f (t - iT)) - \overline{B}_{k,i} \sin(2\pi k \Delta f (t - iT))] g_i(t) \quad (1)$$

[1] In practice, a cyclic prefix [9], [10] would be added to the data block before transmission to eliminate interblock interference and to make the linear convolution with the channel look like a circular convolution. To simplify our notation, we ignore this complication since it does not change the main results of our jitter analysis.

where $\overline{A}_{k,i} = g_k A_{k,i}$, $\overline{B}_{k,i} = g_k B_{k,i}$, and $g_i(t)$ is a rectangular window function defined as

$$g_i(t) = \Pi\left(\frac{t - iT - T/2 + T/(2N)}{T}\right)$$
$$\Pi(t) = \begin{cases} 1, & |t| < 0.5 \\ 0, & |t| > 0.5. \end{cases} \quad (2)$$

In forming the limits of the summation in (1), we have assumed that the Nyquist bin is not used. The transmitted signal $s(t)$, formed by sending a sequence of DMT symbols, is

$$s(t) = \frac{2}{\sqrt{N}} \sum_{i=-\infty}^{\infty} \sum_{k=1}^{N/2-1} [\overline{A}_{k,i} \cos(2\pi k \Delta f t) - \overline{B}_{k,i} \sin(2\pi k \Delta f t)] g_i(t). \quad (3)$$

The signal is sent over the channel where it is convolved with the channel impulse response $h(t)$, yielding a received signal of

$$r(t) = \sum_{i=-\infty}^{\infty} h(t) * \frac{2}{\sqrt{N}} \sum_{k=1}^{N/2-1} [\overline{A}_{k,i} \cos(2\pi k \Delta f t) - \overline{B}_{k,i} \sin(2\pi k \Delta f t)] g_i(t). \quad (4)$$

To focus solely on the effect of timing jitter in this initial discussion, we ignore the contribution of additive noise; the noise will be included after the final expressions are obtained. Denoting the Fourier transform of the channel impulse response by $\mathcal{F}\{h(t)\} = H(f)e^{j\psi(f)}$, we may simplify (4) by making use of the relationship [11]

$$h(t) * [g_0(t) \cos(2\pi k \Delta f t)] \approx H(k\Delta f) g_0(t - \beta(k\Delta f)) \cdot \cos(2\pi k \Delta f t + \psi(k\Delta f)) \quad (5)$$

where $\beta(f) = (-1/2\pi)(\partial\psi(f)/\partial f)$ is the group delay of the channel. A similar expression is obtained for the sine function. For our purposes, the possibility of interblock interference may be eliminated by assuming the group delay to be equal to a constant, which we conveniently take to be zero. In a well-designed DMT system, this approximation will be valid since interblock interference would otherwise be detrimental to system performance. Hence, under these assumptions, the final expression for the received analog DMT signal is given by

$$r(t) = \frac{2}{\sqrt{N}} \sum_{i=-\infty}^{\infty} \sum_{k=1}^{N/2-1} [H_k \overline{A}_{k,i} \cos(2\pi k \Delta f t + \psi_k) - H_k \overline{B}_{k,i} \sin(2\pi k \Delta f t + \psi_k)] g_i(t) \quad (6)$$

where $H_k = H(k\Delta f)$ and $\psi_k = \psi(k\Delta f)$.

At the input to the receiver in Fig. 2, the first step of demodulation is to sample the signal at a nominal rate of $f_s = N\Delta f$. We denote the sampling instances by $(iN + m)T_s + \tau_{m,i}, m \in \{0, 1, \cdots, N-1\}$, where $\tau_{m,i}$ is a timing offset that may vary from sample to sample and $T_s = 1/f_s$. Hence, the received sequence of samples is given by

$$\begin{aligned} r((iN+m)T_s + \tau_{m,i}) &= \frac{2}{\sqrt{N}} \sum_{i=-\infty}^{\infty} \sum_{k=1}^{N/2-1} \\ &\cdot [H_k \overline{A}_{k,i} \cos(2\pi k(iN+m)/N + 2\pi k \Delta f \tau_{m,i} + \psi_k) \\ &- H_k \overline{B}_{k,i} \sin(2\pi k(iN+m)/N + 2\pi k \Delta f \tau_{m,i} + \psi_k)] \\ &\cdot g_i((iN+m)T_s + \tau_{m,i}). \end{aligned} \quad (7)$$

The statistics of the timing error depend upon the timing recovery mechanism used in the DMT system. For simplicity, we assume that synchronization is maintained by using a second-order digital phase-locked loop (DPLL) to track a pilot carrier located at frequency $f_p = p\Delta f$. The pilot signal is generated by sending a fixed constellation point on the pth tone, and the DPLL is updated at the DMT symbol rate. With the DPLL model, a good approximation is that the phase error on the pilot is Gaussian distributed [12], and we define the *phase jitter*, σ_ϕ, as the standard deviation of this Gaussian process.

Next, the received sequence given in (7) is partitioned into blocks of N samples, each of which is transformed by the FFT to obtain an estimate of the transmitted constellation points. To ensure there is no contribution from the past or previous blocks into a sample obtained during the current symbol and, thus, to maintain a reasonable error rate, we must have $\max\{|\tau_{m,i}|/T\} < 1/(2N)$. Another way of stating this is that the peak timing offset should be less than one-half the sampling period. For example, the DMT parameters for an ADSL system that loop times to the central office include a sampling rate of 2.208 MHz, a pilot carrier of 276 kHz, and an FFT size of 512 [13]. With these values, the criteria becomes $\max\{|\tau_{m,i}|\} < 226$ ns, corresponding to a peak phase error of 22.5° on the pilot. Hence, we can safely assume that the group of N samples, $\{r_{m,i}, m = 0, \cdots, N-1\}$, obtained during the ith symbol period is given by

$$\begin{aligned} r_{m,i} = \frac{2}{\sqrt{N}} \sum_{k=1}^{N/2-1} & H_k \overline{A}_{k,i} \\ & \cdot \cos(2\pi km/N + 2\pi k \Delta f \tau_{m,i} + \psi_k) \\ & - H_k \overline{B}_{k,i} \sin(2\pi km/N + 2\pi k \Delta f \tau_{m,i} + \psi_k). \end{aligned} \quad (8)$$

At this point, assumptions regarding the dependence of $\tau_{m,i}$ on the block index i and the intrablock index m must be made to allow for further analysis. Since the DPLL is updated at the DMT symbol rate, the simplest approach would be to assume that $\tau_{m,i}$ is constant over each block and thus independent of m. A more complicated analysis that more closely approximates reality models the change in timing error between consecutive updates as a ramp L samples long followed by a constant for $N - L$ samples, where L depends upon the control voltage bandwidth of the voltage controlled oscillator (VCO) that is part of the phase-locked loop or $L = N$ for a frequency offset. Both cases are considered in the next section.

III. Uncoded DMT Jitter Performance

A. Fixed Offset Over DMT Symbol

For the case in which the timing error is assumed to be fixed over the DMT symbol, we replace $\tau_{m,i}$ with τ_i and compute the discrete Fourier transform (DFT) of (8) to obtain

$$R_{l,i} = g_l H_l e^{j\psi_l} (A_{l,i} + jB_{l,i}) e^{j2\pi l \Delta f \tau_i} \quad (9)$$

as an expression for the detected complex point in the lth bin during the ith symbol period. The complex multiplicative factor $g_l H_l e^{j\psi_l}$ in (9) is a constant that depends upon the channel characteristic and may be compensated by a one-tap frequency domain equalizer (FEQ) in the receiver. Hence, the final expression for the received point is

$$\hat{S}_l = (A_l + jB_l) e^{j2\pi l \Delta f \tau} + (n_{I,l} + jn_{Q,l}) \quad (10)$$

where the noise term $(n_{I,l} + jn_{Q,l})$ included in (10) is a complex Gaussian random variable with $E\{n_{I,l}^2\} = E\{n_{Q,l}^2\} = \sigma_n^2$. The noise variance *after* the FEQ is independent of frequency since the DMT system is designed for equal probability of error across all subchannels and the received constellation on each tone has a normalized minimum distance of 1.0 after FEQ scaling. In obtaining (10), we have dropped the DMT symbol index i to signify that the statistics of the variables in (10) are time-invariant.

To compute the two–dimensional (2-D) error rate performance of the DMT system, we make use of the small angle approximation $e^{j\phi} \approx (1 + j\phi)$ to obtain

$$\hat{S}_l \approx (A_l - B_l 2\pi l \Delta f \tau + n_{I,l}) + j(B_l + A_l 2\pi l \Delta f \tau + n_{Q,l}). \quad (11)$$

Hence, the probability of a correct decision on the lth tone given the transmitted constellation point $A_{q,l} + jB_{q,l}$ and the

phase error $\theta_l = 2\pi l \Delta f \tau$ is

$$P_{c|A_{q,l},B_{q,l},\theta_l} = \left[1 - Q\left(\frac{0.5 - B_{q,l}\theta_l}{\sigma_n}\right) - Q\left(\frac{0.5 + B_{q,l}\theta_l}{\sigma_n}\right)\right] \cdot \left[1 - Q\left(\frac{0.5 - A_{q,l}\theta_l}{\sigma_n}\right) - Q\left(\frac{0.5 + A_{q,l}\theta_l}{\sigma_n}\right)\right] \quad (12)$$

where $q \in \{0, 1, \cdots, 2^{b_l} - 1\}$ is a constellation label and $Q(\cdot)$ represents the Gaussian probability of error function. Since θ_l is related to the phase error on the pilot signal by a constant scaling factor, the 2-D error rate on the lth tone may be written in terms of the phase jitter σ_ϕ as

$$P_{2D|l} = 1 - \int_{-\infty}^{\infty} \frac{f_p}{\sigma_\phi f_l \sqrt{2\pi}} e^{-\theta_l^2 f_p^2 / 2 f_l^2 \sigma_\phi^2} P_{c|\theta_l,l}\, d\theta_l \quad (13)$$

where

$$P_{c|\theta_l,l} = \frac{1}{2^{b_l}} \sum_{q=0}^{2^{b_l}-1} P_{c|A_{q,l},B_{q,l},\theta_l}. \quad (14)$$

The overall 2-D error rate, obtained by averaging over the index l, is given by

$$P_{2D} = \frac{1}{u} \sum_{l \in \mathcal{U}} P_{2D|l} \quad (15)$$

where $\mathcal{U}$ denotes the set of indices corresponding to subchannels used for transmission and $u = |\mathcal{U}|$.

The uncoded DMT system's error rate performance as predicted by (15) will be determined by the poorest performing subchannels. Moreover, (13) and (14) indicate that for a particular level of timing jitter, two main factors determine the error rate performance on the lth tone. The first factor is the frequency of the bin, with higher frequencies experiencing greater levels of jitter than lower frequencies. The second is the size of the constellation supported by the lth bin, where larger constellations are more susceptible to jitter. Fortunately for applications such as ADSL, the higher frequencies typically support smaller constellations than the lower frequencies because of the increase in channel attenuation with frequency.

B. DMT Examples

We now investigate the implications of (15) for the two bit distributions presented in Fig. 3. In both cases, 1616 b are contained in each DMT symbol, and a pilot carrier is located at 276.0 kHz, hence, the null in the bit distributions at this frequency. Scenario A corresponds to transmission over a 9 kft (2.7 km), 26 AWG loop in the presence of near-end crosstalk (NEXT) from ten digital subscriber line (DSL) disturbers and 24 high bit-rate DSL (HDSL) disturbers, and NEXT and far-end crosstalk (FEXT) from ten ADSL disturbers [14]. Scenario B also corresponds to transmission over a 9 kft (2.7 km), 26 AWG loop, but in the presence of NEXT from one T1 disturber in an adjacent wire bundle.

To obtain both bit distributions, we used the practical bit and power allocation algorithm provided in [15]. This

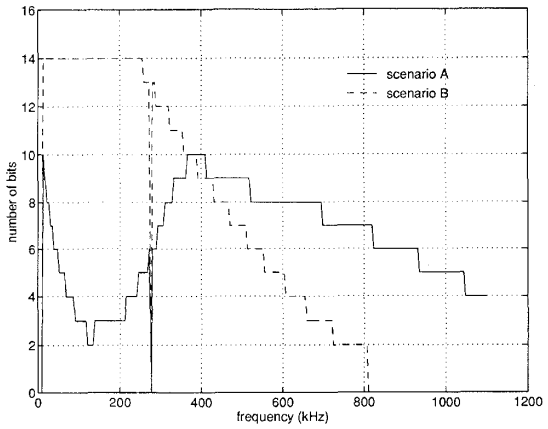

Fig. 3. Uncoded bit distributions for two ADSL scenarios.

algorithm attempts to find for a fixed data rate the integer bit distribution that maximizes system margin under a total power constraint. The algorithm starts with a flat power distribution and iteratively solves the set of equations

$$b_k = \log_2\left(1 + \frac{\mathrm{SNR}_k}{\Gamma \gamma_m}\right)$$
$$b = \sum_{k=1}^{N/2-1} b_k$$
$$b_k \in \{0, 2, 3, \cdots, b_{\max}\}$$

where SNR_k is the SNR on the kth subchannel, Γ is a constant that depends upon the target error rate, γ_m is the margin, and $b_{\max}$ is the maximum number of bits allowed on a subchannel. At the completion of the iterative part of the algorithm, the power on each subchannel is adjusted slightly to ensure equal error rate performance. See [15] for further details. We ran the algorithm on Scenarios A and B with $b_{\max} = 14, \Gamma = 9.8$ dB, and a power constraint of 20.0 dBm.

Figs. 4 and 5 present plots of the uncoded error rate curves obtained for the bit distributions in Fig. 3 at various levels of jitter[2]; square and cross constellations were used on the subchannels in obtaining these results. The continuous curves in the graphs have been obtained by evaluating (15), while the asterisks represent Monte Carlo simulation points obtained by simulating DMT modulation with timing recovery. A solid error rate curve is included in each plot to signify the performance of a system with perfect synchronization.

The correspondence between the theoretical error rate curves and the simulation points in Figs. 4 and 5 verifies the accuracy of the analysis for a wide range of jitter levels. In addition, these plots indicate the importance of choosing a narrow enough DPLL bandwidth or large enough pilot SNR to ensure acceptable error rate performance for a given bit distribution. For instance, although Scenario A results in bits being placed at high frequencies where the jitter is worse,

[2]Error rate curves are plotted versus the normalized SNR, which is proportional to $1/\sigma_n^2$.

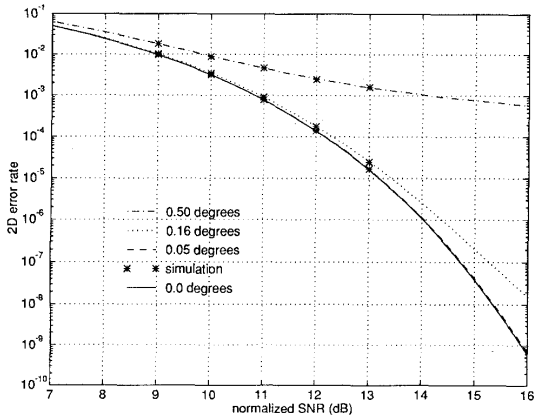

Fig. 4. Uncoded DMT system's error rate performance for Scenario A at various jitter levels.

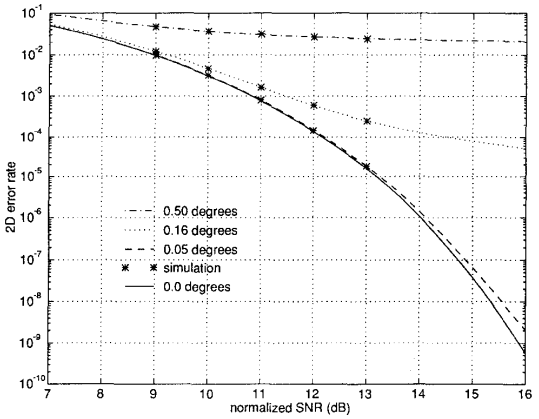

Fig. 5. Uncoded DMT system's error rate performance for Scenario B at various jitter levels.

Scenario B is less tolerable to timing jitter because of the very large constellations used on some of the tones.

Further insight into the degradation in performance caused by timing jitter is presented in Fig. 6 where we plot the 2-D error rate versus the jitter level for normalized SNR's of 11.0 dB and 14.0 dB. This figure clearly illustrates the greater intolerance to timing jitter in Scenario B as compared to Scenario A. In addition, we observe that timing jitter is more critical at lower error rates since the importance of this form of impairment relative to additive noise is greater than at higher error rates. By using the results in Fig. 6, we can determine the maximum tolerable phase jitter for both DMT scenarios and both normalized SNR's to ensure less than a factor of two degradation in the overall error rate. These critical levels are listed in Table I along with the jitter levels required to ensure less than a factor of two degradation on the *worst* tone in the system.[3] As is evident from the table, the jitter requirements are quite stringent for both scenarios.

[3]The jitter level for Scenario A at a normalized SNR of 11.0 dB ($P_{2D} \approx 10^{-3}$) is beyond the range of the plot in Fig. 6.

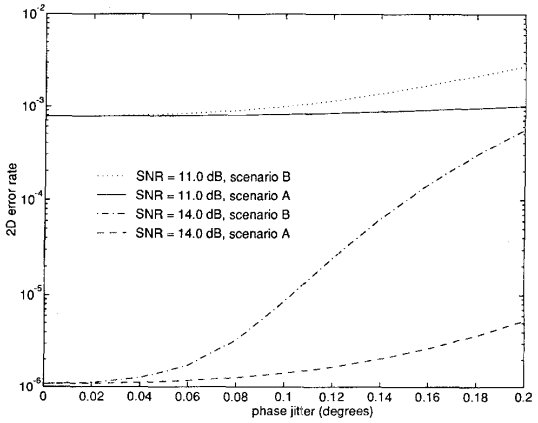

Fig. 6. Error rate versus phase jitter for two DMT scenarios and two normalized SNR's.

TABLE I
JITTER LEVELS REQUIRED TO CAUSE A FACTOR OF TWO DEGRADATION IN ERROR RATE

scenario	uncoded $\sigma_{\phi,max}$ (worst tone)	uncoded $\sigma_{\phi,max}$ (Figure 6)	trellis coded $\sigma_{\phi,max}$ (Figure 9)
B, $\sim 10^{-3}$	0.075°	0.15°	0.10°
A, $\sim 10^{-3}$	0.19°	0.31°	0.22°
B, $\sim 10^{-6}$	0.036°	0.066°	0.067°
A, $\sim 10^{-6}$	0.090°	0.14°	0.16°

C. Variable Offset Over DMT Symbol

The assumption of a constant timing offset over each DMT symbol is equivalent to assuming that the output phase of the VCO changes instantaneously when the control voltage is changed. In practice, the VCO will have a control voltage bandwidth that is determined by a single-pole Butterworth filter. Hence, we model the timing offset as

$$\tau_{m,i} = \begin{cases} \tau_{i-1} + (\tau_i - \tau_{i-1})m/L, & m = 0, \cdots, L-1 \\ \tau_i, & m = L, \cdots, N-1 \end{cases} \quad (16)$$

where L is the number of samples corresponding to one time constant of the filter's impulse response. By allowing $L = N$, we also have a model for the case in which the transmit and receive clocks are offset in frequency. Substituting (16) into (8), we find that the block of received samples representing the ith DMT symbol is given by (17), see equation at the bottom of the next page, where $\overline{\tau}_i = \Delta f \tau_i, \overline{\tau}_{i-1} = \Delta f \tau_{i-1}$, and $\Delta\overline{\tau}_i = \overline{\tau}_i - \overline{\tau}_{i-1}$.

In the Appendix, we evaluate the DFT of (17) to derive an expression for $R_{l,i}$, the received point in the lth bin

$$R_{l,i} = \sum_{k=1}^{N/2-1} H_k(\overline{A}_{k,i} C_{k,l,i} + j\overline{B}_{k,i} D_{k,l,i}) \quad (18)$$

DOCKET ALARM

Explore Litigation Insights

Docket Alarm provides insights to develop a more informed litigation strategy and the peace of mind of knowing you're on top of things.

Real-Time Litigation Alerts

Keep your litigation team up-to-date with **real-time alerts** and advanced team management tools built for the enterprise, all while greatly reducing PACER spend.

Our comprehensive service means we can handle Federal, State, and Administrative courts across the country.

Advanced Docket Research

With over 230 million records, Docket Alarm's cloud-native docket research platform finds what other services can't. Coverage includes Federal, State, plus PTAB, TTAB, ITC and NLRB decisions, all in one place.

Identify arguments that have been successful in the past with full text, pinpoint searching. Link to case law cited within any court document via Fastcase.

Analytics At Your Fingertips

Learn what happened the last time a particular judge, opposing counsel or company faced cases similar to yours.

Advanced out-of-the-box PTAB and TTAB analytics are always at your fingertips.

API

Docket Alarm offers a powerful API (application programming interface) to developers that want to integrate case filings into their apps.

LAW FIRMS
Build custom dashboards for your attorneys and clients with live data direct from the court.

Automate many repetitive legal tasks like conflict checks, document management, and marketing.

FINANCIAL INSTITUTIONS
Litigation and bankruptcy checks for companies and debtors.

E-DISCOVERY AND LEGAL VENDORS
Sync your system to PACER to automate legal marketing.